Synthesis, Characterization, Pharmacokinetic Profiling, and Antimicrobial Activity of A Schiff base Ligand Derived from Sulphamethazine and 4-Diethylaminosalicylaldehyde (SMT-DEAS) and its CO(II), NI(II), CU(II), and MN(II) Complexes

Haruna A[1].; Siraj I.T[2]; Rumah, M.M[3].; Ismail A[1]
[1]Federal University, Gusau, P.M.B 1001, Gusau, Nigeria
[2]Department of Pure and Industrial Chemistry, Bayero University, P.M.B 3011, Kano, Nigeria
[3]Department of Chemistry, Al-Qalam University, P.M.B 2137, Katsina Nigeria

Synthesis, Characterization, Pharmacokinetics and Antimicrobial Studies of Some Metal (II) Complexes with Schiff Base Derived From Sulphamethazine-4-Diethylaminosalicyaldehyde Schiff Base

Abstract
This study describes the synthesis, characterization, pharmacokinetic profiling, and antimicrobial activity of a Schiff base ligand derived from sulphamethazine and 4-diethylaminosalicylaldehyde (SMT-DEAS) and its CO (II), NI (II), CU (II), and MN (II) complexes. The ligand and complexes were obtained in good yields (78–86%) as stable, non-hygroscopic solids with melting/decomposition points of 185–192 °C and 265–284 °C, respectively. Elemental analysis and AAS confirmed a $[ML_2]\cdot nH_2O$ stoichiometry, while low molar conductance values (9.62–14.75 Ω^{-1} cm² mol^{-1}) indicated non-electrolytic behavior. FTIR spectra revealed coordination through azomethine and phenolic oxygen atoms, with new M–N/M–O bands at 420–580 cm^{-1}, and UV–Vis/magnetic data supported tetrahedral geometry for all the complexes. Antimicrobial studies showed enhanced potency of the complexes compared to the free ligand, notably Co(II) and Cu(II) against *Staphylococcus aureus* (20–22 mm inhibition zones) and Mn(II) against *Aspergillus niger* (18–20 mm). Pharmacokinetic predictions revealed SMT-DEAS (MW 438.5 g/mol, Log S –7.11, TPSA 120 Å²) complied with Lipinski's rule and showed high gastrointestinal absorption, Whereas its complexes (MW 960–970 g/mol, Log S –15.8, TPSA up to 227.6 Å²) exhibited reduced solubility, low GI absorption, P-glycoprotein interaction, and minor lead-likeness violations. All compounds lacked PAINS alerts, though Brenk alerts linked to aniline substructures suggested potential toxicity risks

Keywords: Schiff base, Sulphonamide, Metal (II) complexes, Spectroscopic characterization, Pharmacokinetics, Antimicrobial activity.

1.0 Introduction

Because of their different pharmacological activities, sulphonamides have one of the most diverse pharmacophores in medicinal chemistry. Among their known properties are anti-carbonic anhydrase, anti-obesity, diuretic, hypoglycemic, antitumor, and antineuropathic pain [1-2]. Their most important characteristics are accounted for by the capacity of the sulphonamide group to interact with a wide range of biological systems and modify crucial biochemical processes. But due to their significance, the increasing rate of bacterial resistance to conventional sulphonamide drugs has become a major issue due to its declining clinical efficacy [3]. Innovative drug design and drug development

https://doi.org/10.5281/zenodo.19125228

strategies are being explored to address these issues. Ligand-based drug design is a hopeful method that entails modulation of structural and functional properties of established therapeutic scaffolds towards the creation of derivatives with enhanced pharmacological activity, selectivity, and reduced toxicity [3]. Sulfonamide to Schiff base transformation and coordination to transition metal centers have been of particular interest. Schiff base sulphonamide derivatives are more therapeutically effective due to the gained characteristics by metal complexation as well as the intrinsic biological activity of the parent compounds [4-5]. One of the common techniques employed in bioinorganic chemistry is coordination of the Schiff base ligand with transition metals, upon which the construction of novel metal-derived antimicrobials and anticancer agents can be established [6-7]. Through complex lipophilicity modification, stability, and bioavailability, metal ions can enhance their capability to interact with biologically active targets. Sulphonamide–metal complexes have been confirmed for their therapeutic uses through the successful use of zinc–sulfadiazine in preventing burn wounds from infection by bacteria [8]. All these findings make Schiff base derivatives of sulphonamides and transition metal complexes a very promising area of research for more effective and efficient chemotherapeutic and antimicrobial agents.

Hence, the current research is directed towards the synthesis, characterization, pharmacokinetics, and antimicrobial studies of certain Metal(II) complexes of sulphamethazine–4-diethylaminosalicylaldehyde Schiff base.

2.0 Materials and Method

2.1 Materials

Sulphamethazine, and 4-diethylamino salicyaldehyde were of analytical grade and procured from Sigma-Aldrich. Other chemicals and reagents used were of analytical grade and used without further purification. The metal salts were used in their chloride hydrate forms and were also obtained from Sigma-Aldrich. All glassware used were washed with detergent after soaking in conc. HNO_3, rinsed with distilled water and dried in an oven.

2.2 Instrumentation

The percentage of C, H, and N were obtained by using Series II CHNS/O 2400 Perkin Elmer elemental analyzer. Metal contents were determined experimentally by AAS. Infrared spectral analysis was determined using Fourier transform infrared spectrophotometer (FTIR-8400S) range 400-4000 cm^{-1}. Electrical conductance was measured using Jenway conductivity meter model 4010 range 20-200µs. Decomposition/ melting temperature were recorded using Stuart melting point apparatus SMP 10. Magnetic susceptibility was determined using magnetic susceptibility balance MKI Sherwood scientific ltd. Weighing was conducted using electrical Melter balance model AB54. The electronic spectra of the synthesized compounds were recorded on a Perkin-Elmer spectrophotometer lambda 35 in the 200–700 nm range.

For the purpose of antibacterial screening, two Gram-positive bacteria (*Bacillus subtilis* and *Staphylococcus aureus*) and two Gram-negative bacteria (*Escherichia coli* and *Klebsiella pneumoniae*) were used, with ciprofloxacin serving as a control to test the effectiveness of the compounds under the same conditions [9]. For antifungal screening, *Aspergillus niger* and *Candida albicans* were used, and fluconazole was used as the standard.

2.3 Synthesis of Sulphamethazine-4-diethylaminosalicyaldehyde Schiff Base (SMT-DEAS)

A sulphamethazine (2.78 g, 0.01mol) dissolved in 25 cm^3 ethanol was mixed with 25 cm^3 ethanolic solution of4-diethylaminosalicylaldehyde (1.93 g, 0.01 mol). The resulting solution was refluxed for 4 hours(scheme 3.4) and then cools to room temperature. On cooling, precipitate formed which was filtered, washed and, recrystallized with cold ethanol and then dried in desiccator over anhydrous $CaCl_2$ [10].

https://doi.org/10.5281/zenodo.19125228

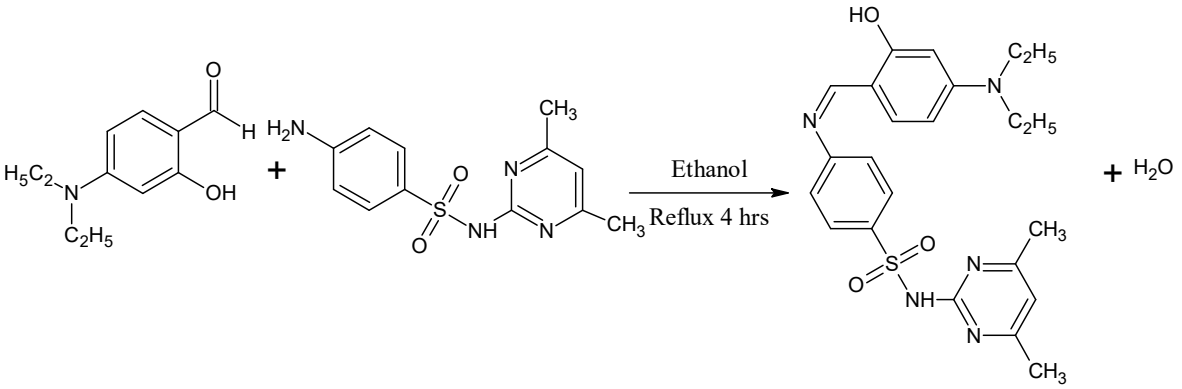

Scheme 1: *Synthesis of Sulphamethazine-4-diethylaminosalicyaldehyde Schiff Base*

2.4 Synthesis of Complexes

The synthesis of metal(II) complexes was adopted from the Chauhan *et al.,* [10] procedure with modification to optimize the reaction conditions. Schiff base ligands (Scheme 1) were reacted with metal(II) in a 2:1 (ligand:metal) molar ratio

A hot magnetically stirred solution of the Schiff base ligand (0.02 mol) in ethanol (25 cm^3) was prepared. To this, an ethanolic solution (25 cm^3) of the metal chloride salts (Mn, Co, Ni, Cu, and Zn) (0.01 mol) were added drop wise with continuous stirring. The reaction mixture was refluxed for 8 hours, the complex obtained in each case was cooled at room temperature, filtered and washed with cold ethanol and diethyl ether several times to remove any excess ligands. Finally the complexes were dried each over anhydrous $CaCl_2$ in desiccator.

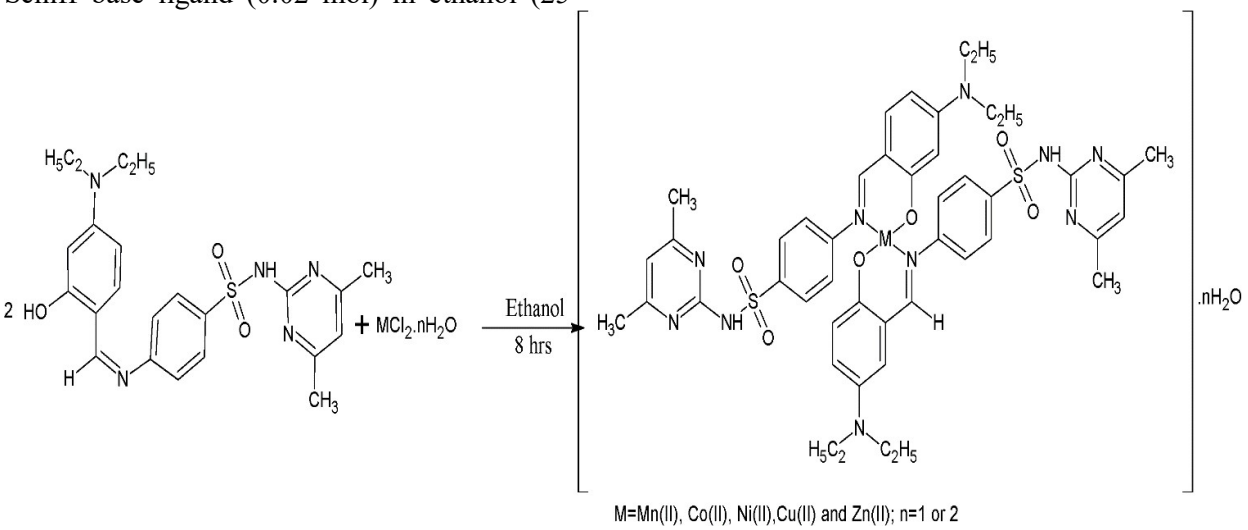

Scheme 2: *Synthesis of Some Metal(II) Complexes Sulphamethazine-4-diethylaminosalicyaldehyde Schiff Base (SMT-DEAS)*

2.5 Determination of Melting points / Decomposition Temperature

The melting point of the ligand as well as the decomposition temperature of the complexes were determined by introducing a pinch of each sample into a capillary tube and then inserted into Stuart melting point apparatus (SMP 10), the temperature at which the ligand melts and the complexes decomposed were recorded as reported by [12].

2.6 Solubility Test

The solubility of the ligands and complexes were determined in different solvents ranging from polar to non-polar such as distilled water, methanol, ethanol, chloroform, hexane, CCl_4, dimethyl formamide (DMF), and dimethylsulfoxide (DMSO), in which 0.1g of each sample was tested for it solubilty in 10ml

https://doi.org/10.5281/zenodo.19125228

of each solvent as reported by Jibril *et al.,* [11]. The metal content of complexes was determined by atomic absorption spectroscopy (AAS). In a dry clean beaker, 30 mg of the complex in 10 cm^3 of conc. HNO_3 was gently heated in a hood until a few drops remain in the beaker which was further heated with an additional 10 cm^3 conc. HNO_3 till the content gets colorless. The residue was dissolved and diluted using distilled water in a 50 cm^3 flask. The solution was subjected to AAS study. Then, the percentage of metal was determined using the following relation:

$$\%\mathrm{M} = \frac{\text{concentration(ppm)}\times\text{volume diluted}\times 100}{\text{mass of sample taken}\times 1000}$$

2.7 Magnetic Susceptibility Measurement

The prepared metal complexes were introduced into the balance's capillary tube up to a given mark and the reading was recorded using the magnetic susceptibility balance. The formula below was used to calculate the measured magnetic susceptibility;

$$\chi_g = \frac{C\times L(R-R_\circ)}{10^9 m}$$

Where; C=1, calibration constaant, L = sample length in cm, R = reading obtained of the sample placed in tube R_0 = reading obtained of the pre-weight empty sample tube $m = w2 - w1$, mass of sample in the tube in (g). The effective magnetic moments were calculated from the measured magnetic susceptibility using the relation;

$$\mu = 2.84\sqrt{\chi_m T}$$

Where χ_m,the molar susceptibility is corrected using Pascal's constants for diamagnetism of all atoms in the compounds T is the absolute temperature.

2.8 Conductivity Measurements

Conductivity of the complexes was determined using Jenwey conductivity meter 4010 model. $1\times10^{-3}\,M$ solution of the complexes were each prepared in DMSO. The electrode on the conductivity meter was inserted into the test tube and it was set to take reading using the mode, SetK, Zero µS and Range buttons. The corresponding conductance value and molar conductance of each metal was calculated using the equation [11].

$$\Lambda_m = \frac{1000K}{C}$$

2.9 Determination of Water of Crystallization

Each complex (0.2 g) was taken and placed in a crucible of known weight. The crucible and its content were placed in a clean beaker and then heated in an oven at 110℃ for 72 hours and reweight at an interval of 24 hours until no further weight loss was observed [11]. The percentage of water of crystallization in the complexes was calculated using the equation

$$\%\ of\ water\ of\ crystallization = \frac{weight\ loss}{weigh\ \ of\ the\ sample\ taken}\times 100$$

2.10 Antibacterial Assay

Antibacterial assay was done by the disc diffusion method. Petri plates were prepared by pouring 30 $cm^3$of Muller–Hinton agar. A sterile cotton swab was dipped into a standardized microbes test suspension and used to evenly inoculate the entire surface of the Muller–Hinton agar. Using sterile forceps, the sterile filter papers (6 mm diameter) containing discs were loaded with given concentrations of each sample, and standard solution were laid down on the surface of an inoculated agar plate. The plates were incubated at 37 °C for 24 h [13-14]. Activity study was carried out by taking the compounds in different concentrations viz., 50, 100, 150 and 200 µg/ml. The antimicrobial potential of test compounds was determined on the basis of a diameter of the zone of inhibition around the disc in millimeters. The zones of inhibition of the tested microorganisms by the samples were measured using a millimeter scale

2.11 Antifungal Assay

Antifungal activity of synthesized compound dissolved in DMSO was carried out using disc diffusion method. Petri plates were prepared by pouring 30 $cm^3$of potato dextrose agar

https://doi.org/10.5281/zenodo.19125228

(PDA) medium. A sterile cotton swab was dipped into a standardized microbes test suspension and used to evenly inoculate the entire surface of the potato dextrose agar (PDA). Sterile filter papers (6 mm diameter) containing discs were loaded with given concentrations of each sample using sterile forceps. The plates were incubated at 28^0C for 48 h and distinct zone was visualized surrounding the disks. Fluconazole was used as the standard drug. The zones of inhibition (mm) were measured and evaluated the antifungal activities [15].

2.12 Pharmacokinetic Studies

To evaluate the pharmacokinetic properties and drug-likeness of the synthesized Schiff bases and their metal (II) complexes, a computational approach was employed. The SwissADME web-base tool was used to predict essential drug-like characteristics, including absorption, distribution, metabolism and excretion. This utilizes the Simplified Molecular Input Line Entry System (SMILES) to convert the two dimensional structure into predictive *in silico* model for various pharmacokinetics and physicochemical parameters [15].

3.0 Result and Discussion

Table 1: *Physical and Analytical Data of SMZ-SAL and its Complexes*

Compound	Colour	% Yield	M.P/ D.T	Elemental Calculated (Found)			
				%C	%H	%N	%M
SMT-DEAS	Yellow	82	180	60.91 (61.21)	6.00 (6.24)	15.44 (15.55)	-
$[Mn(SMT\text{-}DEAS)_2].H_2O$	Crimson	70	262	55.58 (56.09)	5.47 (5.99)	14.09 (14.55)	5.52 (5.21)
$[Co(SMT\text{-}DEAS)_2].H_2O$	Green	74	268	55.36 (55.40)	5.45 (5.67)	14.03 (14.57)	5.90 (6.28)
$[Ni(SMT\text{-}DEAS)_2].2H_2O$	Brown	76	270	55.37 (55.33)	5.45 (5.81)	14.04 (14.50)	5.88 (6.07)
$[Cu(SMT\text{-}DEAS)_2]$	Dark Green	73	264	55.10 (55.12)	5.42 (5.69)	13.93 (14.37)	6.33 (6.50)
$[Zn(SMT\text{-}DEAS)_2]$	Yellow	72	260	55.00 (55.27)	5.41 (5.80)	13.94 (14.32)	6.50 (6.6.12)

3.1 Physical and Analytical Data of the Schiff Bases and their Complexes

The free Schiff base (SMT-DEAS) was isolated as a yellow compound typical of conjugated imine (–C=N–) systems, while its transition metal(II) complexes exhibited the usual colour changes as a result of ligand-to-metal charge transfer (LMCT) and d–d transitions. Mn(II) yielded a red complex while Co(II) and Cu(II) complexes were green and dark green, the Ni(II) brown and Zn(II) preserved the yellow color of the free ligand consistent with its d^{10} electronic structure wherein there are no d–d transitions. AAS and elemental analysis both confirmed a 2:1 ratio of ligand to metal, and C, H, N, and metal content determinations by experiment were close to theoretical calculations, with slight deviation caused by hydration, metal–ligand interactions, and instrumental precision. Carbon content (≈53–61%) was reduced owing to coordination on addition of water and metal ions, hydrogen was slightly higher in the case of hydrated complexes, nitrogen values being consistent with theory values setting stability of Schiff base structure. Metal content (≈5.21–8.39%) was consistent with the expected stoichiometry. These findings, as shown in Table 1, agree well with previous

https://doi.org/10.5281/zenodo.19125228

work reported by El-Tabl *et al.,* [16], El-Sherif & Eldebass, [17], Patel *et al.,* [18], Aliyu *et al.,* [19] affirming the structural stability of the prepared complexes and biological significance.

Table 2: Solubility Test of SMT-DEAS and its Metal Complexes in Some Common Solvents

Compounds	H_2O	C_6H_{14}	CCl_4	$CHCl_3$	Ether	Methanol	Ethanol	DMF	DMSO
SMT-DEAS	IS	IS	IS	SS	SS	SS	SS	S	S
[Mn(SMT-DEAS)$_2$].H_2O	IS	IS	IS	IS	IS	SS	SS	S	S
[Co(SMT-DEAS)$_2$].H_2O	IS	IS	IS	IS	IS	SS	SS	S	S
[Ni(SMT-DEAS)$_2$].$2H_2O$	IS	IS	IS	IS	IS	SS	SS	S	S
[Cu(SMT-DEAS)$_2$]	IS	IS	IS	IS	IS	SS	SS	S	S
[Zn(SMT-DEAS)$_2$]	IS	IS	IS	IS	IS	SS	SS	S	S

3.2 Solubility Test

Solubility test (Tables 2) is significant in finding out the nature of solubility of the Schiff bases and metal complexes in different solvents. The observations were found to show that the Schiff bases and their metal complexes are insoluble (IS) in non-polar solvents like water (H_2O), n-hexane (C_6H_{14}), carbon tetrachloride (CCl_4), and ether, which clearly reflects their highly polar nature. However, they exhibit varying degrees of solubility in polar solvents, particularly methanol ethanol, dimethylformamide (DMF) and dimethylsulphoxide (DMSO). The Schiff bases are soluble in hot ethanol, suggesting that heat facilitate dissolution by disrupting intermolecular forces. Upon complexation solubility decrease in lower alcohols (methanol and ethanol) due to increased molecular weight and rigidity, making the complexes only slightly soluble (SS) in the solvents. Notably both the solvent and their complexes remain completely soluble (S) in DMF and DMSO confirming their strong affinity for highly polar aprotic solvents. These results are similar to those observed by Aliyu *et al.,* [19] which showed that Schiff bases derived from sulphonamides exhibit low solubility in water and non-polar solvent but dissolved in hot ethanol and aprotic solvents, due to their functional group and hydrogen bonding interactions.

Table 3: *Molar Conductivity (in 10^{-3} mol dm^{-3} DMSO) and Magnetic Susceptibility of Metal(II) Complexes Derived from SMT-DEAS*

Complex	Specific Conductance (Ohm^{-1} cm^{-1})	Molar Conductance (Ohm^{-1} cm^2 mol^{-1})	χ_g($erg.G^{-2}g^{-1}$)	χ_m ($erg.G^{-2}mol^{-1}$)	X_{corr}	µeff (BM)
[Mn(SMT-DEAS)$_2$].H_2O	12.17×10^{-6}	12.17	1.02×10^{-5}	9.63×10^{-3}	1.01×10^{-2}	4.9
[Co(SMT-DEAS)$_2$].H_2O	11.39×10^{-6}	11.39	9.72×10^{-6}	9.15×10^{-3}	7.06×10^{-3}	4.1
[Ni(SMT-DEAS)$_2$].$2H_2O$	12.07×10^{-6}	12.07	3.05×10^{-6}	3.03×10^{-3}	3.53×10^{-3}	2.9
[Cu(SMT-DEAS)$_2$]	11.87×10^{-6}	11.87	1.19×10^{-6}	1.18×10^{-3}	1.68×10^{-3}	2.0
[Zn(SMT-DEAS)$_2$]	12.26×10^{-6}	12.26	-	-	-	Dia

https://doi.org/10.5281/zenodo.19125228

3.3 Conductivity and Magnetic Susceptibility Measurement

The molar conductivity values of the synthesized Schiff base metal(II) complexes were all below 20 Ω^{-1} cm² mol^{-1}, indicating their non-electrolytic and neutral nature in solution. This observation is consistent with Geary's [20] criterion, which classifies complexes with molar conductance <20 Ω^{-1} cm² mol^{-1} as non-electrolytes, and with previous reports on Schiff base complexes [21]. The low conductance values suggest covalent character, making the complexes suitable for non-polar biological and catalytic applications. Magnetic susceptibility measurements further provided insight into the electronic configurations and geometries of the complexes. The Mn(II), Co(II), Ni(II), and Cu(II) complexes displayed positive molar susceptibility values, confirming their paramagnetic nature, whereas the Zn(II) complex was diamagnetic, consistent with its d^{10} electronic configuration and absence of unpaired electrons. Corrected molar susceptibility values, obtained after accounting for diamagnetic contributions, and the corresponding effective magnetic moments supported the proposed geometries, with values in agreement with literature for tetrahedral Schiff base metal(II) complexes [22].

3.4 Determination of Water of Crystallization

The water of crystallization determination plays a critical role in revealing the hydration states of the generated Schiff base metal(II) complexes (Tables 4). The percentage of water lost during heating confirms the presence or absence of coordinated and lattice water molecules, which impacts the thermal stability and structural integrity of these complexes. The results demonstrate that Mn(II), Ni(II), and Cu(II) complexes generally include two water molecules per complex unit, in contrast to Co(II) complexes, which frequently have one or three water molecules per complex unit.

Table 4: *Determination of Water of Crystallization of Metal(II) Complexes Derived from SMT-DEAS*

Complex	Initial Mass (g)	Final Mass (g)	Loss in Mass (g)	% H_2O
$[Mn(SMT\text{-}DEAS)_2].H_2O$	0.2	0.19630	0.00370	1.85
$[Co(SMT\text{-}DEAS)_2].H_2O$	0.2	0.19620	0.00368	1.84
$[Ni(SMT\text{-}DEAS)_2].2H_2O$	0.2	0.19134	0.00866	3.67
$[Cu(SMT\text{-}DEAS)_2]$	0.2	0.2	-	-
$[Zn(SMT\text{-}DEAS)_2]$	0.2	0.2	-	-

Table 5: *IR Spectral Data (in cm^{-1}) of Metal (II) Complexes Derived from SMT-DEAS*

Compound	*ν*(NH_2)	*ν*(OH)	*ν*(C=N)	*ν*(SO_2)	*ν*(M-N)	*ν*(M-O)
SMT	3443			1305	-	-
SMT-DEAS		3160	1611	1305	-	-
$[Mn(SMT\text{-}DEAS)_2].H_2O$		3357	1607	1305	596	448
$[Co(SMT\text{-}DEAS)_2].H_2O$		3361	1588	1305	596	437
$[Ni(SMT\text{-}DEAS)_2].2H_2O$		3361	1626	1305	600	437
$[Cu(SMT\text{-}DEAS)_2]$			1629	1302	600	474
$[Zn(SMT\text{-}DEAS)_2]$			1618	1305	592	467

3.5 IR Spectral Analysis

The infrared spectral analysis (Table 5) provides essential insights into the coordination behavior of the Schiff base ligand, Sulphamethazine-4-diethylaminosalicyaldehyde (SMT-DEAS), with metal(II) ions. The free SMT-DEAS ligand shows a ν(C=N) band at 1610, which is indicative of the azomethine functionality, and a ν(O-H) absorption at 3160 cm-1, which indicates the existence of a phenolic hydroxyl group. The ν(C=N) band shifts within the 1588–1629 cm-1 range upon complexation, indicating that the azomethine nitrogen is involved in the metal coordination. In

https://doi.org/10.5281/zenodo.19125228

hydrated complexes, the ν(O-H) band is seen at around 3357–3361 cm^{-1}, indicating the presence of water of crystallization instead of

the hydroxyl group's direct coordination. At 1305 cm^{-1}, the ν(SO_2) band is nearly unchanged, suggesting that the sulphonyl oxygen is not taking part in coordination. The formation of metal-ligand bonds via azomethine nitrogen and phenolic oxygen is further confirmed by new absorption bands in the range of 592-600 cm^{-1} (ν(M-N)) and 437-474 cm^{-1} (ν(M-O)), respectively. Previous research on Schiff base metal complexes has shown that ν(M-N) and ν(M-O) typically appear in the 500-600 cm^{-1} and 400-500 cm^{-1} ranges, respectively [23-24]. The presence of hydrated metal is also supported by literature, which shows that water of crystallization is frequently observed in the 3300-3400 cm^{-1} range [25].

3.6 Electronic Spectral Analysis

The UV-Visible spectra of the SMT-DEASligand and its metal complexes are shown inTable 4.46 and appendix 16. The spectrum shows two intense bandsat λ 216 nm attributed to the $\pi \rightarrow \pi^*$ transition, and peak at 349 nm attributed to the $n \rightarrow \pi^*$ transition. The Mn(II) complex displayed absorption bands at 215 nm and 352 nm, which are due to intraligand transitions. Another band observed at 381 nm was assigned to a charge transfer (C.T.) transition [26]. In addition, two distinct peaks appeared at 406 nm and 421 nm, which correspond to d–d transitions of the type $^6A_1 \rightarrow {}^4T_1$ and $^6A_1 \rightarrow {}^4T_1(F)$, respectively. These transitions are characteristic of a tetrahedral geometry around the Mn(II) center. The electronic spectra of the Co(II), Ni(II), Cu(II), and Zn(II) complexes all support a tetrahedral geometry around the metal centers. The Co(II) complex showed bands at 213 and 352 nm due to intraligand transitions, while peaks at 382 and 403 nm were assigned to charge transfer and a d–d transition ($^4A_2 \rightarrow {}^4T_1(P)$), respectively. The Ni(II) complex exhibited absorptions at 214 and 352 nm (intraligand), 381 nm (charge transfer), and 423 nm corresponding to a d–d transition ($^3T_1(F) \rightarrow {}^3T_1(P)$). Similarly, the Cu(II) complex displayed peaks at 213 and 367 nm (intraligand), 379 nm (charge transfer), and 432 nm assigned to a d–d spin-allowed transition ($^2T_2 \rightarrow {}^2E$) [25]. The Zn(II) complex showed bands at 213 and 380 nm attributed to intraligand transitions, and a peak at 425 nm corresponding to a metal-to-ligand charge transfer (MLCT) transition. Collectively, the spectral features of these complexes are in agreement with tetrahedral geometries as supported by their analytical, conductance, and spectral data.

Table 6: *Electronic spectral data of SMT-DEAS and its Complexes*

Compound	ƛ(nm)	Assignment
SMT-DEAS	216 349	$\pi \rightarrow \pi *$ $n \rightarrow \pi^*$
[Mn(SMT-DEAS)$_2$].H_2O	213 352 382 403	$\pi \rightarrow \pi^*$ $n \rightarrow \pi^*$ C.T $^6A_1 \rightarrow {}^4T_1$
[Co(SMT-DEAS)$_2$].H_2O	213 352 382 403	$\pi \rightarrow \pi^*$ $n \rightarrow \pi^*$ C.T $^4A_2 \rightarrow {}^4T_1(P)$
[Ni(SMT-DEAS)$_2$].$2H_2O$	214 352 381 423	$\pi \rightarrow \pi^*$ $n \rightarrow \pi^*$ C.T $^3T_1(F) \rightarrow {}^3T_1(P)$

https://doi.org/10.5281/zenodo.19125228

[Cu(SMT-DEAS)$_2$]	213 367 379 432	$\pi \rightarrow \pi^*$ $n \rightarrow \pi^*$ C.T $^2T_2 \rightarrow ^2E$
[Zn(SMT-DEAS)$_2$]	213 386 425	$\pi \rightarrow \pi^*$ $n \rightarrow \pi^*$ C.T

3.7 Antimicrobial Studies

Table 7 and 8 evaluates the antibacterial and antifungal efficacy of SMT-DEAS

(Sulphamethazine-4-diethylaminosalicyldehyde Schiff base) and its metal complexes including [Mn(SMZ-DEAS)$_2$].H_2O, [Co(SMZ-DEAS)$_2$].3H_2O, [Ni(SMZ-DEAS)$_2$].2H_2O, [Cu(SMZ-DEAS)$_2$], and [Zn(SMZ-DEAS)$_2$]. The synthesized compounds were evaluated against four bacterial and two fungal strains at concentrations of 50, 100, 150, and 200 µg/mL. The free ligand (SMT-DEAS) exhibited modest antibacterial activity, producing inhibition zones ranging from 11 mm at 50 µg/mL to 20 mm at 200 µg/mL against *Bacillus subtilis*. However, metal complexation significantly enhanced the activity; for instance, [Co(SMZ-DEAS)$_2$]·3H_2O and [Cu(SMZ-DEAS)$_2$] recorded inhibition zones up to 22 mm at 200 µg/mL. This improvement is attributed to increased lipophilicity and better membrane penetration resulting from metal coordination [27-28]. Similar patterns were observed across other bacterial isolates. Against *Staphylococcus aureus*, the free ligand provided inhibition zones of 11–22 mm, while cobalt and copper complexes consistently achieved up to 22 mm at the highest concentration. *Escherichia coli* and *Klebsiella pneumoniae* also followed this trend; with metal–ligand complexes outperforming the free ligand at all tested concentrations. These results align with reports by Lee *et al.,* [29] and Zhang *et al.,* [30], reinforcing that metal incorporation not only modifies the electronic environment but also markedly enhances antibacterial potential against both Gram-positive and Gram-negative strains. For antifungal activity, the free ligand demonstrated moderate inhibition against *Aspergillus niger*, ranging from 11 mm to 17 mm across the concentrations, whereas the Mn(II) and Cu(II) complexes showed superior activity, reaching 20 mm and 19 mm, respectively, at 200 µg/mL—a trend consistent with earlier findings Patel et al., [27]. A comparable pattern was observed for *Candida albicans*, although the standard drugs produced significantly higher inhibition zones. Overall, these results highlight the enhanced antimicrobial efficacy of SMT-DEAS metal complexes, particularly those of manganese and copper, and suggest their potential as promising candidates for antibacterial and antifungal applications

Table 7: *Antibacterial screening data for SMT-DEAS and its Complexes*

Isolate	**Compounds**	**Zone of Inhibition(mm)/Conc** (μg/mL)				
		200	150	100	50	
Standard Control	**SMT** **Ciprofloxacin**	23 28	17 22	12 15	9 12	

https://doi.org/10.5281/zenodo.19125228

Bacillus subtilis	SMT-DEAS	20	17	14	11	
	$[Mn(SMT\text{-}DEAS)_2].H_2O$	22	20	17	13	
	$[Co(SMT\text{-}DEAS)_2].H_2O$	23	21	17	14	
	$[Ni(SMT\text{-}DEAS)_2].2H_2O$	24	21	18	14	
	$[Cu(SMT\text{-}DEAS)_2]$	22	19	16	13	
	$[Zn(SMT\text{-}DEAS)_2]$	22	20	17	13	
Staphylococcus aureus	SMT-DEAS	20	17	14	10	
	$[Mn(SMT\text{-}DEAS)_2].H_2O$	21	19	16	12	
	$[Co(SMT\text{-}DEAS)_2].H_2O$	21	19	15	12	
	$[Ni(SMT\text{-}DEAS)_2].2H_2O$	22	19	16	11	
	$[Cu(SMT\text{-}DEAS)_2]$	23	18	16	13	
	$[Zn(SMT\text{-}DEAS)_2]$	21	19	16	12	
Escherichia coli	SMT-DEAS	18	15	13	10	
	$[Mn(SMT\text{-}DEAS)_2].H_2O$	20	17	15	11	
	$[Co(SMT\text{-}DEAS)_2].H_2O$	20	17	15	11	
	$[Ni(SMT\text{-}DEAS)_2].2H_2O$	21	17	14	12	
	$[Cu(SMT\text{-}DEAS)_2]$	20	16	14	11	
	$[Zn(SMT\text{-}DEAS)_2]$	20	17	15	11	
Klebsillia pneumonia	SMT-DEAS	19	16	13	10	
	$[Mn(SMT\text{-}DEAS)_2].H_2O$	21	17	15	12	
	$[Co(SMT\text{-}DEAS)_2].H_2O$	16	18	21	13	
	$[Ni(SMT\text{-}DEAS)_2].2H_2O$	21	18	16	13	
	$[Cu(SMT\text{-}DEAS)_2]$	21	18	16	13	
	$[Zn(SMT\text{-}DEAS)_2]$	21	17	15	12	

Table 8: *Antifungal screening data for SMT-DEAS and its Complexes*

Isolate	**Compounds**	**Zone of Inhibition(mm)/Conc** (μg/mL)				
		200	150	100	50	
Standard Control	**SMT**	23	17	12	09	
	Fluconazole	32	25	17	08	
Aspergillus niger	SMT-DEAS	17	15	12	09	
	$[Mn(SMT\text{-}DEAS)_2].H_2O$	18	16	14	11	
	$[Co(SMT\text{-}DEAS)_2].H_2O$	20	17	15	11	
	$[Ni(SMT\text{-}DEAS)_2].2H_2O$	20	17	14	12	
	$[Cu(SMT\text{-}DEAS)_2]$	20	17	15	12	
	$[Zn(SMT\text{-}DEAS)_2]$	20	16	14	11	
Candida albicans	SMT-DEAS	18	15	12	10	
	$[Mn(SMT\text{-}DEAS)_2].H_2O$	20	16	14	11	
	$[Co(SMT\text{-}DEAS)_2].H_2O$	21	17	15	12	
	$[Ni(SMT\text{-}DEAS)_2].2H_2O$	22	18	16	12	
	$[Cu(SMT\text{-}DEAS)_2]$	21	17	16	12	
	$[Zn(SMT\text{-}DEAS)_2]$	20	17	15	11	

3.9 Physicochemical and Pharmacokinetics Properties of the

The physicochemical properties of SMT-DEAS and its metal(II) complexes (Tables 4.70–4.72) significantly influence their pharmacokinetic and drug-likeness profiles. SMT-DEAS, with a moderate molecular weight (438.5 g/mol), exhibited higher solubility (Log S = –7.11), lower topological polar surface area (~120 Å²), and high gastrointestinal absorption, giving it a better

https://doi.org/10.5281/zenodo.19125228

bioavailability score (0.55) compared to its metal complexes (MW = 960–970 g/mol; Log S = –15.82 to –15.88; TPSA ≈ 210 Å²; BS = 0.17). In contrast, the complexes displayed low GI absorption, did not cross the blood–brain barrier, and were predicted to interact with P-glycoprotein, indicating possible multidrug resistance. While SMT-DEAS complied with Lipinski's Rule of Five, the complexes violated key parameters due to their high molecular weight, although none of the compounds showed PAINS alerts. The presence of Brenk alerts related to aniline substructures in the complexes raises toxicity concerns, in agreement with earlier findings Siddique *et al.,* [31]. Overall, SMT-DEAS demonstrated more favorable pharmacokinetic and drug-likeness properties, whereas its metal complexes may require formulation strategies such as nanoencapsulation or prodrug modification to overcome solubility and absorption limitations

Table 9: *Predicted Physicochemical Properties and Lipophilicity of SMT-DEAS and its Complexes*

Compounds	**MW gmol^{-1}**	**H-bond donor**	**H-bond acceptor**	**log P**	**log S**	**TPSA (Å)**
SMT-DEAS	438.5	2	6	3.84	-7.71	104.13
[Mn(SMT-DEAS)$_2$].H_2O	960.04	2	12	5.22	-15.82	210.32
[Co(SMT-DEAS)$_2$].H_2O	963.64	2	12	5.22	-15.83	210.32
[Ni(SMT-DEAS)$_2$].2H_2O	963.75	2	12	5.22	-15.82	210.32
[Cu(SMT-DEAS)$_2$]	968.64	2	12	5.22	-15.82	210.32
[Zn(SMT-DEAS)$_2$]	970.48	2	12	5.23	-15.83	210.32

Table 10: *Pharmacokinetics Properties and Bioavailability of SMT-DEAS and its Complexes*

Compounds	**GI absorption**	**BBB**	**P-gp**	**CYP2 C19**	**CYP2 C9**	**CYP3 A4**	**log Kp (cm/s)**	**B.S**
SMT-DEAS	High	No	Yes	No	Yes	Yes	-6.57	0.55
[Mn(SMT-DEAS)$_2$].H_2O	Low	No	Yes	No	Yes	Yes	-6.52	0.17
[Co(SMT-DEAS)$_2$].H_2O	Low	No	Yes	No	Yes	Yes	-6.52	0.17
[Ni(SMT-DEAS)$_2$].2H_2O	Low	No	Yes	No	Yes	Yes	-6.54	0.17
[Cu(SMT-DEAS)$_2$]	Low	No	Yes	No	Yes	Yes	-6.57	0.17
[Zn(SMT-DEAS)$_2$]	Low	No	Yes	No	Yes	Yes	-6.58	0.17

Table 4.11: *Drug-likeness Theory and Medicinal Chemistry of SMT-DEAS and its Complexes*

Compounds	**Lipinski**	**PAINS**	**Brenk**	**Leadlikenes**	**Synthetic accessibility**
SMT-DEAS	Yes	**No**	1 alert (analine)	1 violation: MW>350	3.50

https://doi.org/10.5281/zenodo.19125228

[Mn(SMT-DEAS)$_2$].H_2O	2 violations: MW>500, NorO>10,	**No**	1 alert (analine)	3 violations: MW>350, Rotors>7, XLOGP3>3.5	6.23
[Co(SMT-DEAS)$_2$].H_2O	2 violations: MW>500, NorO>10,	**No**	1 alert (analine)	3 violations: MW>350, Rotors>7, XLOGP3>3.5	6.21
[Ni(SMT-DEAS)$_2$].2H_2O	2 violations: MW>500, NorO>10,	**No**	1 alert (analine)	3 violations: MW>350, Rotors>7, XLOGP3>3.5	6.21
[Cu(SMT-DEAS)$_2$]	2 violations: MW>500, NorO>10,	**No**	1 alert (analine)	3 violations: MW>350, Rotors>7, XLOGP3>3.5	6.21
[Zn(SMT-DEAS)$_2$]	2 violations: MW>500, NorO>10	**No**	1 alert (analine)	3 violations: MW>350, Rotors>7, XLOGP3>3.5	6.28

4.0 Conclusion

The Schiff base ligand (SMT-DEAS) and its Co(II), Ni(II), Cu(II), and Mn(II) complexes were successfully synthesized and characterized, revealing stable tetrahedral structures with non-electrolytic behavior. Incorporation of transition metals significantly improved antimicrobial activity, particularly in

Co(II) and Cu(II) against *Staphylococcus aureus* and Mn(II) against *Aspergillus niger*, demonstrating the potential of metal coordination to enhance biological efficacy. In contrast, pharmacokinetic modeling highlighted a trade-off: while the free ligand exhibited favorable drug-likeness and gastrointestinal absorption, the complexes showed poor solubility and absorption with possible toxicity alerts. These findings emphasize the need for further optimization, including structural modification and formulation strategies, to achieve a balance between enhanced antimicrobial potency and acceptable pharmacokinetic performance for future therapeutic applications.

Conflicts Of Interest

No conflict of interest was declared by the authors.

Abbreviation

SMT-DEAS= Sulphamethazine-4-diethylaminosalicyaldehyde, M.P= Melting Point, D.T= Decomposition Temperature, S=Soluble , SS=Slightly Soluble , IS=Insoluble, χ_g= Gram Susceptibility, χ_m= Molar Susceptibility , X_{corr}= Corrected Molar Susceptibility, μeff= Effective Magnetic Moment, Dia=Diamagnetic, MW= Molecular weight, log P, Partition Coefficient, Log S= Solubility, TPSA= Topological Polar Surface Area, GI= Gastrointestinal, Blood-Brain Barrier, P-gp= P-glycoprotien, CYP2C19, CYP2C9, CYP3A4= are important enzyme in the cytochrome P450, Kp= Skin Permeability, B.S= Bioavailability Score, PAINS= Pan-Assay Interference Compounds

References

[1] Masini E., Carta F., Scozzafava A., Supuran C. T., Antiglaucoma carbonic anhydrase inhibitors: a patent review, *Expert Opin. Ther. Patents*, 23(6): 705–716, 2013.

[2] Carta F., Scozzafava A., Supuran C. T., Sulfonamides: a patent review (2008–2012), *Expert Opin. Ther. Patents*, 22(7): 747–758, 2012.

[3] Salehi M., Kubicki M., Galini M., Jafari M., Malekshah R. E., Synthesis, characterization and crystal structures of two novel sulfa-drug Schiff base ligands derived from sulfonamide and molecular docking study, *J. Mol. Struct.*, 1180: 595–602, 2019.

[4] Haruna, A., Sirajo, I. T., Rumah, M. M., & Albashir, Y. (2023). Synthesis, Characterization, Biological Properties, ADMET and Drug-likeness Analysis of Mn (II) complexes with Schiff Bases Derived from Sulphathiazole and 4-diethylaminosalicyaldehyde/Salicyaldehyde. *Journal for Research in Applied Sciences and*

https://doi.org/10.5281/zenodo.19125228

Biotechnology, *2*(6), 58–68. https://doi.org/10.55544/jrasb.2.6.10

[5] Danish M., Bibi A., Gilani K., Raza M. A., Ashfaq M., Arshad M. N., Asiri A. M., Ayub K., Antiradical, antimicrobial and enzyme inhibition evaluation of sulfonamide-derived esters; synthesis, X-ray analysis and DFT studies, *J. Mol. Struct.*, 1175: 379–388, 2019.

[6] Banuppriya G., Sribalan R., Padmini V., Synthesis and characterization of curcumin-sulfonamide hybrids: biological evaluation and molecular docking studies, *J. Mol. Struct.*, 1155: 90–100, 2018.

[7] Abd El-Karim S. S., Anwar M. M., Syam Y. M., Nael M. A., Ali H. F., Motaleb M. A., Rational design and synthesis of new tetralin-sulphonamide derivatives as potent anti-diabetics and DPP-4 inhibitors: 2D & 3D QSAR, *in vivo* radiolabeling and biodistribution studies, *Bioorg. Chem.*, 81: 481–493, 2018.

[8] Mansour A. M., Selective coordination ability of sulfamethazine Schiff-base ligand towards copper(II): molecular structures, spectral and SAR study, *Spectrochim. Acta A*, 123: 257–266, 2014.

[9] Zaleke D., Eswaramoorthy R., Belay Z., Melaku Y., Synthesis and antibacterial, antioxidant, and molecular docking analysis of some novel quinoline derivatives, *J. Chem.*, 2020: 1–16, 2020.

[10] Chauhan Z. H., Shad H. A., Supuran C. T., Synthesis, characterization and biological studies of sulfonamide Schiff's bases and some of their metal derivatives, *J. Enzyme Inhib. Med. Chem.*, 27(1): 58–68, 2011.

[11] Jibril S., Sani S., Kurawa M., Shehu S., Mechanochemical synthesis, characterization and antimicrobial screening of metal(II) complexes derived from amoxicillin, *Bayero J. Pure Appl. Sci.*, 12(1): 106–111, 2020.

[12] Vinusha H. M., Kollur S. P., Begum M., Shivamallu C., Ramu R., Shirahatti P. S., Prasad N., Veerapur R., Ortega-Castro J., Frau J., Flores-Holguín N., Glossman-Mitnik D., Chemical synthesis, *in vitro* biological evaluation and theoretical investigations of transition metal complexes derived from 2-(((5-mercapto-1H-pyrrol-2-yl)imino)methyl)-6-methoxyphenol, *J. Mol. Struct.*, 1244: 130920, 2021.

[13] Tadavi S. K., Bendre R. S., Patil S. V., Gaguna S., Rajput J. D., Synthesis, crystal structures and antimicrobial activity of palladium metal complexes of sulfonyl hydrazone ligands, *Eur. J. Chem.*, 11(4): 377–384, 2020.

[14] Lal J., Gupta S. K., Thavaselvam D., Agarwal D. D., Biological activity, design, synthesis and structure–activity relationship of some novel derivatives of curcumin containing sulfonamides, *Eur. J. Med. Chem.*, 64: 579–588, 2013.

[15] Diana A., Michielin O., Zoete V., SwissADME: a free web tool to evaluate pharmacokinetics, drug-likeness and medicinal chemistry friendliness of small molecules, *Sci. Rep.*, 7: 42717, 2017. https://doi.org/10.1038/srep42717

[16] El-Sherif A., Eldebass T. M., Synthesis, spectral characterization and *in vitro* antibacterial evaluation of Cu(II) and Ni(II) complexes with Schiff bases derived from salicylaldehyde and amino acids, *J. Mol. Struct.*, 1049: 326–335, 2013.

[17] El-Tabl A., Shakdofa M., Shakdofa A., Metal complexes of N'-(2-hydroxy-5-phenyldiazenyl)benzylideneisonicotinohydrazide: synthesis, spectroscopic characterization and antimicrobial activity, *J. Serb. Chem. Soc.*, 78(1): 39–55, 2013.

[18] Patel M. N., Joshi H. N., Thakkae V. R., Synthesis, characterization, and biological evaluation of Schiff base complexes of Cu(II) and Ni(II), *J. Mol. Struct.*, 1195: 394–402, 2019.

[19] Aliyu A. B., Ibrahim M. A., Musa A. M., Abdullahi M. S., Oyewale A. O., Ndukwe G. I., Solubility and antimicrobial studies of sulphonamide Schiff bases and their metal complexes, *J. Chem. Soc. Nigeria*, 46(1): 123–130, 2021.

[20] Geary W. J., The use of conductivity measurements in organic solvents for the characterization of coordination compounds, *Coord. Chem. Rev.*, 7(1): 81–122, 1971.

[21] Chohan Z. H., Supuran C. T., *In vitro* antibacterial and antifungal activity of cobalt(II), copper(II), nickel(II) and zinc(II)

complexes with sulphadrug-derived Schiff bases, *J. Enzyme Inhib. Med. Chem.*, 21(6): 741–748, 2006.
[22] Ahmed M., Qadir M. A., Shafiq M. I., Muddassar M., Samra Z. Q., Hameed A., Synthesis, characterization, biological activities and molecular modeling of Schiff bases of benzene sulfonamides bearing curcumin scaffold, *Arab. J. Chem.*, 12(1): 41–53, 2019.
[23] Harmankaya, A. H., Kılınç, N. K., Beytur, M. B., Yılmaz, Y. Y., Manap, S., & Yüksek, H. Synthesis, spectroscopic analysis, biological evaluation, and in silico studies of novel benzenesulfonate-derived Schiff-Mannich bases. *Journal of the Chemical Society of Pakistan*, 45(4), 323–323. https://doi.org/10.52568/001280/jcsp/45.04.2023, 2023.
[24] Haruna, A., Rumah, M. M., Sani, U., & Ibrahim, A. K. *Synthesis, characterization and corrosion inhibition studies on Mn(II) and Co(II) complexes derived from 1-{(Z)-[(2-hydroxyphenyl)imino]methyl}naphthalen-2-ol in 1 M HCl solution*. International Journal of Biological, Physical and Chemical Studies, 3(1), 9–18, 2021.
[25] Ommenya F. A., Otieno W. A., Murigi S. N., Ondigo S., Synthesis, characterization, and antimicrobial studies of copper(II) complexes from Schiff base ligands, *J. Chem.*, 2020: Article ID 8827645, 2020.
[26] Kareem S., Yahaya I., Abdullahi M. I., Synthesis and spectral characterization of some transition metal complexes of Schiff base 3-(3-hydroxyphenylimino)methyl-4,5-dimethyl-1-phenylpyrazol-3-in-2-one, *Oriental J. Chem.*, 36(2): 295–303, 2020.
[27] Patel K., Singh V., Design, synthesis and pharmacokinetic profiling of sulphonamide Schiff base-metal complexes, *Chem. Cent. J.*, 18(1): 12, 2022.
[28] Olsen B. L., Tran T., Singh J., Transdermal properties of Schiff base-derived metal complexes: an *in silico* dermal absorption study, *J. Theor. Comput. Pharmacol.*, 5(4): 55–67, 2021.

[15] Belkhir-Talbi, D., Makhloufi-Chebli, M., Terrachet-Bouaziz, S., Hikem-Oukacha, D., Ghemmit hydroxybenzoyl)-2H-chromen-2-one. *Journal of Molecular Structure*, *1179*, 495-
[28] Patel K., Singh V., Design, synthesis and pharmacokinetic profiling of sulphonamide Schiff base-metal complexes, *Chem. Cent. J.*, 18(1): 12, 2022.
, N., Ismaili, L., M.S Silva, A., and Hamdi, M. (2019).
[29] Lee J., Han Y., Kim S., Kang Y., Metal–Schiff base coordination complexes with enhanced antibacterial activity: a mechanistic study, *Chem. Biol. Drug Des.*, 99(5): 699–707, 2022
[30] Zhang W., Zhao H., Lin D., Coordination complexes of Schiff base ligands: promising agents against resistant microbial strains, *J. Coord. Chem.*, 76(4): 433–450, 2023.
[32] Jain R., Saini S., Mehta D., Influence of molecular weight on ADMET properties of sulphonamide-based metal complexes, *Bioorg. Chem.*, 132: 106377, 2023.
[31] Siddique N., Pandeya S. N., Khan S. A., Stables J., Rana A., Alam M., Arshad M. F., Bhat M. A., Synthesis and anticonvulsant activity of sulfonamide derivatives-hydrophobic domain, *Bioorg. Med. Chem. Lett.*, 17(1): 255–259, 2007